Biochemical and Biophysical Research Communications 463 (2015) 148–153

Contents lists available at ScienceDirect

Biochemical and Biophysical Research Communications

journal homepage: www.elsevier.com/locate/ybbrc

Absence-like seizures and their pharmacological profile in *tottering-6j* mice

Tae Yeon Kim [a, 1], Takehiro Maki [b, 1], Ying Zhou [c], Keita Sakai [b], Yuri Mizuno [b], Akiyoshi Ishikawa [b], Ryo Tanaka [b], Kimie Niimi [a], Weidong Li [c], Norihiro Nagano [b], Eiki Takahashi [a, c, *]

[a] *Research Resources Center, RIKEN Brain Science Institute, Saitama, 351-0198, Japan*
[b] *Sleep Science Laboratories, HAMRI Co. Ltd., Ibaraki, 306-0128, Japan*
[c] *Bio-X Institutes, Key Laboratory for the Genetics of Developmental and Neuropsychiatric Disorders (Ministry of Education), Shanghai Jiao Tong University, Shanghai, 200240, People's Republic of China*

ARTICLE INFO

Article history:
Received 30 April 2015
Available online 20 May 2015

Keywords:
Antiepileptic drug
Ataxia
Cacna1a
Electroencephalograms
Spike-and-wave discharge
Tottering-6j mice

ABSTRACT

We previously showed that recessive ataxic *tottering-6j* mice carried a base substitution (C-to-A) in the consensus splice acceptor sequence linked to exon 5 of the α_1 subunit of the Cav2.1 channel gene (*Cacna1a*), resulting in the skipping of exon 5 and deletion of part of the S4–S5 linker, S5, and part of the S5–S6 linker in domain I of the α_1 subunit of the Cav2.1 channel. However, the electrophysiological and pharmacological consequences of this mutation have not previously been investigated. Upon whole-cell patch recording of the recombinant Cav2.1 channel in heterologous reconstitution expression systems, the mutant-type channel exhibited a lower recovery time after inactivation of Ca^{2+} channel current, without any change in peak current density or the current–voltage relationship. *Tottering-6j* mice exhibited absence-like seizures, characterized by bilateral and synchronous 5–8 Hz spike-and-wave discharges on cortical and hippocampal electroencephalograms, concomitant with sudden immobility and staring. The pharmacological profile of the seizures was similar to that of human absence epilepsy; the seizures were inhibited by ethosuximide and valproic acid, but not by phenytoin. Thus, the *tottering-6j* mouse is a useful model for studying Cav2.1 channel functions and *Cacna1a*-related diseases, including absence epilepsy.

1. Introduction

The voltage-gated calcium channel (VGCC) is a molecular complex with several subunits: α1, β, $\alpha_2\delta$, and γ [1]. The α1 subunit is essential for channel functionality and determines the basic properties of the channel. The pore-forming transmembrane α1 subunit is organized into four homologous domains (I–IV) with six transmembrane α helices (S1–S6) and a pore-forming P loop between S5 and S6 [2]. Neuronal VGCC mediates several important functions including neurotransmitter release, neuronal excitation, neurite outgrowth, synaptogenesis, neuronal survival, differentiation, plasticity, and regulation of gene expression. This VGCC contains an α1 subunit of the Cav2 family, which includes the Cav2.1 (P/Q-type), Cav2.2 (N-type), and Cav2.3 (R-type) channels [1].

In mutants of the human *CACNA1A*, changes to the pore-forming α1 subunit of the Cav2.1 channel cause several neurological disorders including familial hemiplegic migraine type 1 (FHM1), episodic ataxia type 2 (EA2), spinocerebellar ataxia type 6 (SCA6), and epilepsy [3–5]. As mutations in *CACNA1A* trigger such a wide range of symptoms and disorders, mice with various types of mutation in the *Cacna1a* gene are useful to obtain insights into channel function and disease processes [6]. Mouse Cav2.1α1 mutants include a knockout strain lacking any Cav2.1 current [7] and spontaneous point mutants including *rocker* (*rkr*), *tottering* (*tg*), *rolling Nagoya* (*rol*), *leaner* (*la*), *tottering-4j*, *tottering-5j*, *tottering-6j*, and *wobbly* [1,6]. A spontaneous rat Cav2.1α1 mutant has been termed *groggy* (GRY) [8]. These *Cacna1a* mutants exhibit distinct phenotypes, ranging from mild to severe ataxia and movement disorders. In addition, the *rkr*, *tg*, *tottering-4j*, and *la* mice and GRY

* Corresponding author. Research Resources Center, RIKEN Brain Science Institute, 2-1 Hirosawa, Wako, Saitama, 351-0198, Japan. Fax: +81 48 467 9692.
E-mail address: etakahashi@brain.riken.jp (E. Takahashi).
[1] These authors contributed equally to this work.

http://dx.doi.org/10.1016/j.bbrc.2015.05.050
0006-291X/

rats exhibit absence-like seizures characterized by generalized, bilateral spike-and-wave discharges (SWDs) on electroencephalograms (EEGs), concomitantly with behavioral arrest resembling absence seizures in humans.

We previously described a novel *Cacna1a* mutant, the recessive ataxia *tottering-6j* mouse [9], generated in the Neuroscience Mutagenesis Facility of the Jackson Laboratory (Bar Harbor, MN, USA). *Tottering-6j* mice carry a chemically induced mutation (the mutating agent was ethylnitrosourea [ENU]) that is a base substitution (C-to-A) in the consensus splice acceptor sequence linked to exon 5, which results in skipping of exon 5 and splicing of exon 4 directly to exon 6. The effect of this mutation would be expected to be severe, as the α1 subunit protein lacks a significant part of the S4–S5 linker, S5, and part of the S5–S6 linker of domain I [9]. *Tottering-6j* mice exhibit motor dysfunction in the footprint, rotating rod, and hind-limb extension tests. However, neither the electrophysiological nor the pharmacological consequences of the mutation have yet been investigated.

In the present study, we conducted an electrophysiological analysis and defined the pharmacological profile of *tottering-6j* mice; this mouse line serves as a novel model of human absence epilepsy.

2. Materials and methods

2.1. Animals

This work was approved by the Animal Experiments Committee of RIKEN and HAMRI CO., Ltd (approval nos.: ID: No. H24-2-206 [RIKEN] and 14-H116 [HAMRI CO., Ltd.]). The *tottering-6j* mouse strain, with a mixed C57BL/6J and BALB/cByJ genetic background, was provided by the Jackson Laboratory and was backcrossed with C57BL/6J mice for 12 generations. The mice were allowed *ad libitum* access to water and food pellets (5058 PicoLab Mouse Diet 20; LabDiet, MO, USA) and housed at room temperature (24 ± 3 °C) and 50 ± 20% humidity under a 12:12-h light: dark cycle (light from 8:00 am to 8:00 pm). All tests were performed during the light phase on male mice only.

2.2. In situ hybridization

The brains of mice 36 weeks of age were dissected after perfusion, fixed in Tissue Fixative (Gonostaff, Tokyo, Japan), embedded in paraffin, and sectioned (6-μm-thick slices). The probe was a 691 bp cDNA fragment (nts 6068 to 6748 of Cav2.1α_1 cDNA; Accession Number: NM_007578.3). Hybridization was conducted as previously reported [10].

2.3. Real-time quantitative reverse transcription polymerase chain reaction

Total RNAs were isolated from the olfactory bulb, cerebral cortex, caudate putamen, hippocampus, cerebellum, and liver of mice aged 36 weeks, using the TRIzol reagent (Invitrogen, CA, USA). To quantify the mRNA levels of the gene of interest, we used real-time quantitative reverse transcription polymerase chain reaction (qRT-PCR) coupled with an ABI7700 sequence detection system (Applied Biosystems, CA, USA), as previously reported [11]. The primers used were CT2F (5′-CTGCGCTACTTCGAGATGTG-3′) and CT2R (5′-AACATAGTCAAAATATCGCAGCAC-3′), and the probe was MT2-probe2 (5′-ATCCTCATGGTCATTGCCATGAGCAGCATCGCTCTGGCCGCCGAGGACCCGGTGCAGCCCAACGCACCCC-3′). Each mRNA expression level was calculated relative to that of Cav2.1α_1 mRNA in wild-type mice.

2.4. Transient expression of recombinant Cav2.1 channels in mammalian cells

Human embryonic kidney (HEK) tsA-201 cells (Sigma–Aldrich Corporation, MO, USA) were cultured in Dulbecco's modified Eagle's medium supplemented with 10% (v/v) fetal bovine serum and 0.06% (w/v) kanamycin at 37 °C under 5% (v/v) CO_2. tsA-201 cells were cotransfected with pCMV6-AC-GFP-based recombinant plasmids carrying cDNAs encoding mouse wild-type Cav2.1α_1 (wt, ORIGENE Technologies, Inc., MD, USA) or *tottering-6j*-type Cav2.1α_1 (*6j*, ORIGENE Technologies, Inc.), together with plasmids encoding the mouse β and $\alpha_2\delta$ subunits (ORIGENE Technologies, Inc.). We used the *Trans*IT-X2™ Dynamic Delivery System (Mirus Bio, LLC, WI, USA). After transfection, the cells were held at 28 °C under 5% (v/v) CO_2 for 4–5 days prior to the collection of electrophysiological recordings.

2.5. Whole-cell current recordings

Electrophysiological measurements were performed on tsA-201 cells. All currents were recorded at room temperature using a whole-cell patch clamp technique employing an Axopatch 200B amplifier (Molecular Devices, CA, USA). Signals were digitized with the aid of the ITC-18 interface (Instrutech Corp., NY, USA). Data were collected and analyzed using Axograph 4.6 software (Molecular Devices). Recording pipettes were pulled from micro-glass capillaries (GD-1.5; NARISHIGE Group, Tokyo, Japan) using a micropipette puller (P-97; Sutter Instruments, CA, USA). The resistance of patch electrodes was 2–3 MΩ when they were filled with the pipette solution described below. The series resistance was usually compensated by >70%, and leakage currents were measured during application of four leak-subtraction pre-pulses applied immediately before each test pulse; the leakage was subtracted from the current recorded during the test pulse. All currents were filtered at 3 kHz (low pass) and sampled at 10 or 100 kHz during tail current analyses. Ba^{2+} currents through Ca^{2+} channels were recorded using an external solution that contained 5 mM $BaCl_2$, 40 mM tetraethylammonium chloride (TEA-Cl), 87.5 mM CsCl, 1 mM $MgCl_2$, 10 mM HEPES, and 10 mM glucose (the pH was adjusted to pH 7.2 with TEA-OH). The pipette solution contained 105 mM Cs-methanesulfonate, 25 mM TEA-Cl, 1 mM $MgCl_2$, 10 mM HEPES, 11 mM EGTA, and 4 mM Mg-ATP (the pH was adjusted to pH 7.2 with CsOH).

2.6. Electroencephalograms (EEGs) and behavioral observations

To obtain electroencephalograms (EEGs), *tottering-6j* mice 29–61 weeks of age were anesthetized via intraperitoneal injection of 55 mg/kg pentobarbital sodium salt (Kyoritsuseiyaku Corporation, Tokyo, Japan). A reference screw electrode was implanted in the left side of the skull [Anterior-Posterior (AP) = −1.4 mm/Lateral (L) = 1.75 mm of bregma]. The cortical EEG electrode was implanted in the right side of the skull (AP = 2.2 mm/L = 1.4 mm). The hippocampal EEG electrode was inserted into the hippocampal CA1 area through the right skull [AP = −2.0 mm/L = 1.25 mm/Depth (ventral from the dura mater) = 1.2 mm of bregma]. A miniature plug was positioned and fixed on the midline of the parietal bone to afford an electrical connection. After recovery, mice were moved to a recording cage (23 × 16 × 23 cm^3) placed in an electrically shielded and sound-attenuated room. The implanted electrode of each mouse was connected to a cable; this carried signal output. The mice were allowed to move freely with access to food and water *ad libitum*. After about 24 h of habituation, cortical and hippocampal EEGs were continuously recorded, and behavioral changes observed. EEG signals were amplified (AB-610J, NIHON

KOHDEN CO., Tokyo, Japan), filtered (bandpass 0.5–1 kHz) and digitally recorded (256 Hz/channel) on a computer running recording software (Vital Recorder, KISSEI COMTEC Co., Ltd, Nagano, Japan). Abnormal EEG waveforms such as spike-and-wave discharges (SWDs) were analyzed using NeuroScore (Data Sciences International, MN, USA). A SWD lasting for >1 s was considered an absence-like seizure. When the time interval between two SWDs was <1 s, the discharges were regarded as a single seizure.

2.7. Effects of antiepileptic drugs

The antiepileptic drugs used were 150 mg/kg ethosuximide (ESM; E7138, Sigma–Aldrich Japan, Inc.), 200 mg/kg valproic acid (VPA; P4543, Sigma–Aldrich Japan, Inc.), and 60 mg/kg phenytoin (PHT; 166-12082, Wako Pure Chemical Industries, Ltd., Osaka, Japan). These drug doses were as recommended in previous reports [8,12]. Each antiepileptic drug was dissolved in 0.5% (w/v) methylcellulose (131-17811, Wako Pure Chemical Industries, Ltd.). *Tottering-6j* mice 35–64 weeks of age were habituated over a 24-h period, and the drugs or vehicle were then injected intraperitoneally. Hippocampal EEGs were recorded for 20 min prior to drug administration (reference data) and continuously for 0–20 min, 20–40 min, and 60–80 min after administration. The numbers and durations of SWDs were measured in each 20-min period by reference to the EEG traces. Each animal was given a single dose of one drug (only) on each experimental day.

2.8. Data analysis

Data are presented as means ± standard errors of the means (SEMs). All statistical analyses were performed with the aid of GraphPad Prism Software (CA, USA). Data were analyzed using Dunnett's test or by analysis of variance (ANOVA) followed by Bonferroni's correction for multiple comparisons between groups, if appropriate.

3. Results

3.1. Expression of Cav2.1α_1 mRNA

In situ hybridization (ISH) was used to determine the Cav2.1α_1 expression patterns in wild-type and *tottering-6j* mice; these were very similar (Fig. 1). An antisense probe showed that both strains exhibited widespread expression of the α_1 subunit in the brain, with particularly high-level expression evident in the olfactory bulb, cerebral cortex, caudate putamen, hippocampus, and cerebellar Purkinje cells. The sense probe yielded no signal from any brain. On gross histological examination of the whole brain and cerebellum, the cytoarchitecture of the mutant brain appeared to be normal. We examined the expression levels of $Ca_v2.1\alpha_1$ in the olfactory bulb, cerebral cortex, caudate putamen, hippocampus, cerebellum, and liver of the two strains of mice ($n = 10$/group) via real-time qRT-PCR. The relative expression levels of total Cav2.1α_1 did not significantly differ between strains in any of the olfactory bulb (wild-type and *tottering-6j*: 1.05 ± 0.03 and 1.04 ± 0.07), cerebral cortex (wild-type and *tottering-6j*: 1.01 ± 0.08 and 1.07 ± 0.02), caudate putamen (wild-type and *tottering-6j*: 1.02 ± 0.06 and 1.01 ± 0.03), hippocampus (wild-type and *tottering-6j*: 1.05 ± 0.05 and 1.02 ± 0.04), or cerebellum (wild-type and *tottering-6j*: 1.06 ± 0.05 and 1.02 ± 0.07). Liver fractions from either strain did not yield detectable PCR products.

3.2. Electrophysiological characterization of tottering-6j-type Cav2.1 channels

To explore the functional nature of the *tottering-6j*-type Cav2.1 channel, the electrophysiological properties of mutant (*6j*) and

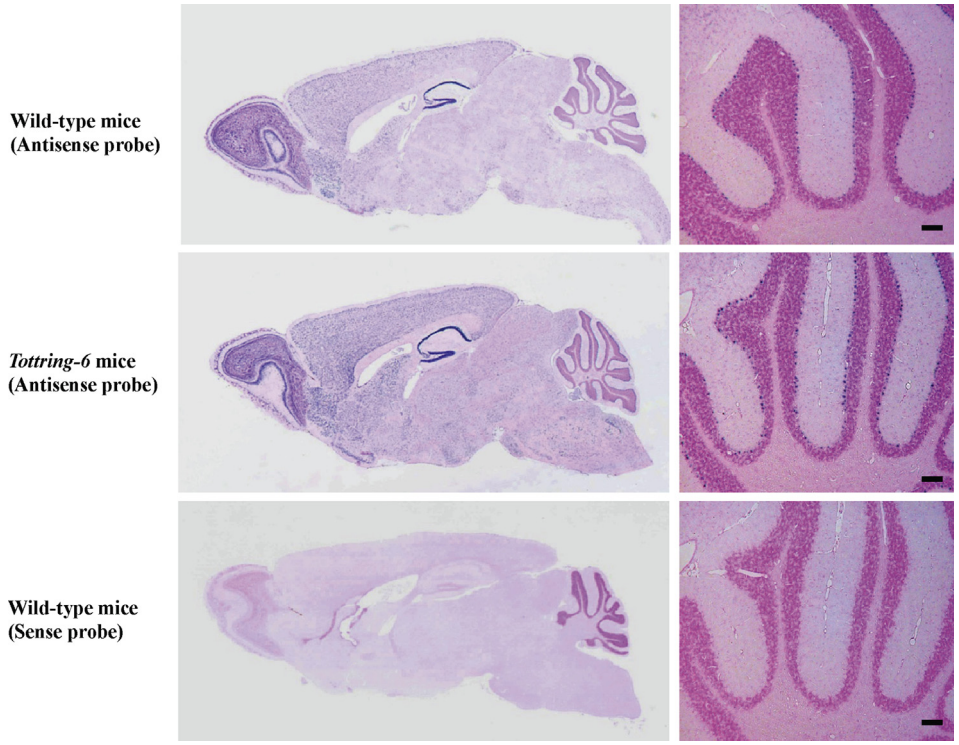

Fig. 1. Expression of Cav2.1α_1 mRNA as revealed by in situ hybridization. Representative sagittal sections of the whole brain and large subpopulations of the cerebella of wild-type ($n = 6$) and *tottering-6j* ($n = 5$) mice. Scale bar: 200 μm.

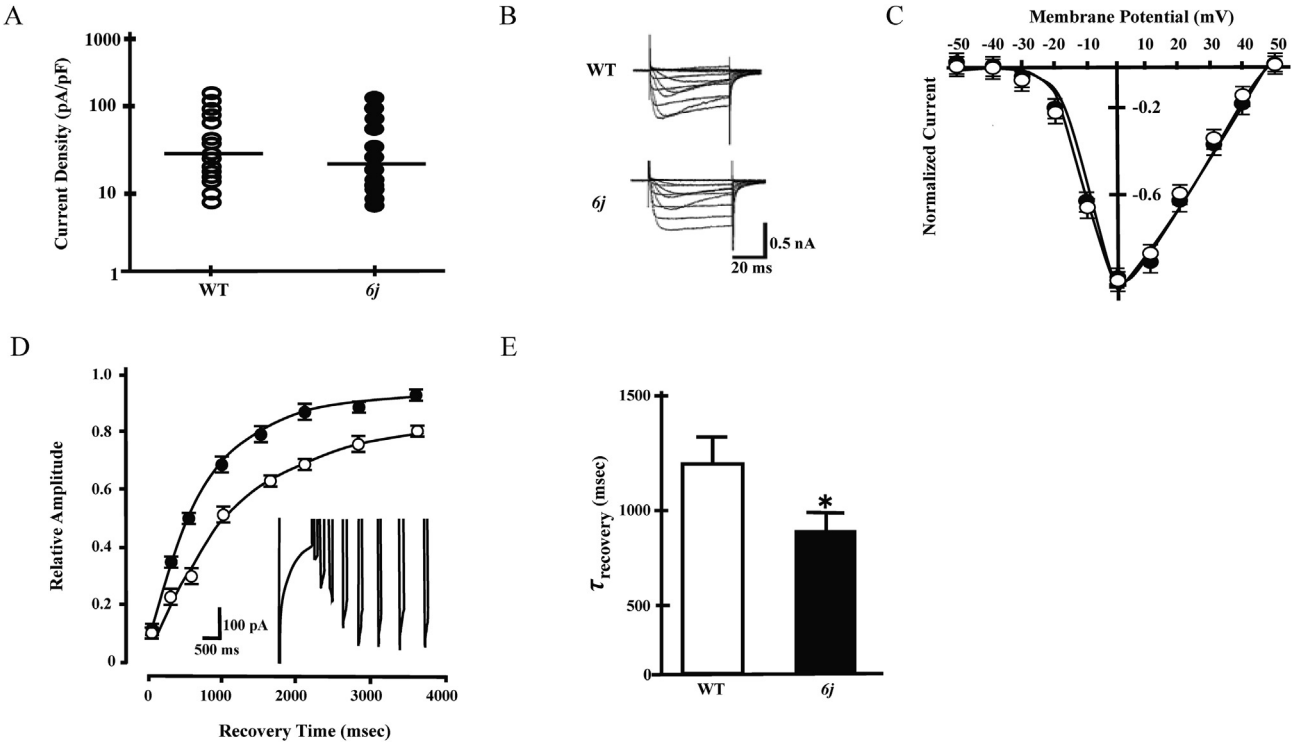

Fig. 2. Ca^{2+} channel currents in HEK tsA-201 cells. The recording bath solution contained 5 mM Ba^{2+} as the charge carrier. (A) Distributions of peak current densities at 0 mV and the geometric means (var) of 15 wild-type and 17 mutant cells. As the data distribution was skewed, raw data were log-transformed to allow statistical comparisons. (B, C) Current–voltage relationships from 9 to 11 experiments, respectively, on wild-type and mutant channels. (B) Representative families of Ba^{2+} currents evoked by 100-ms depolarizing pulses from −50 to 50 mV delivered to the wild-type and mutant channels, at 10-mV increments, from a holding potential of −90 mV. (C) Peak current amplitudes were normalized to the maximum amplitudes and plotted against the membrane potentials. (D, E) Recovery from inactivation after a 1-s depolarization pulse delivered at 0 mV. A 100-ms depolarizing test pulse was applied at various times after the 1-s depolarizing prepulse at 0 mV. (D) Representative currents of mutant-type channels are shown in the inset. The peak amplitudes elicited by the test pulses were normalized to the peak amplitudes of the depolarizing prepulses. The mean values were plotted against recovery intervals and fitted to a single exponential function ($n = 11$ for wild-type channels and $n = 13$ for mutant channels). (E) Average recovery time constants (the $\tau_{recovery}$ values) are shown. Wild-type channels: WT, open circles. Mutant-type channels: *6j*, closed circles. *$p < 0.05$, compared with wild-type channels (Dunnett's test).

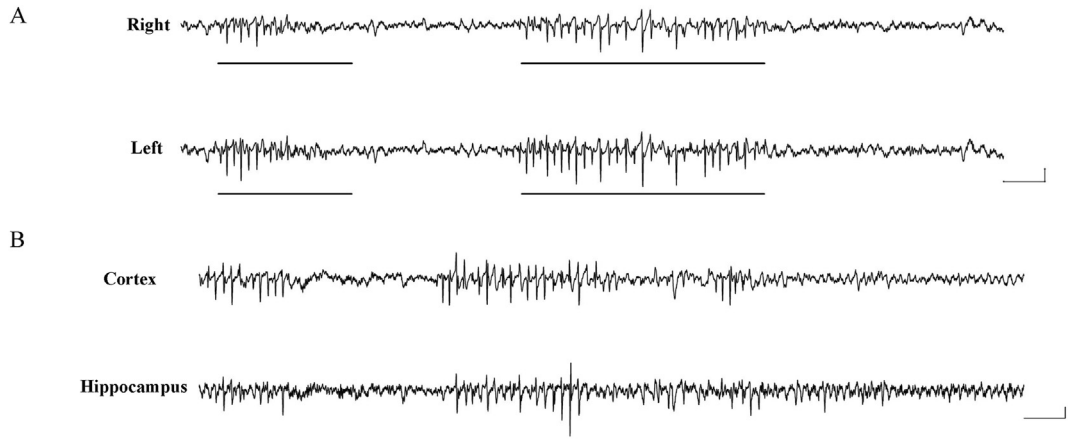

Fig. 3. EEG recordings from *tottering-6j* mice. (A) The right (upper) and left (lower) cortical EEGs exhibited bilateral synchronous 5–8 Hz SWDs concomitant with behavioral arrest (black bar). (B) SWDs occurred synchronously in both the cortex and hippocampus. Calibration: 200 μV and 1 s.

wild-type (wt) channels transiently expressed in HEK tsA-201 cells were compared using the whole-cell patch clamp recording technique. The *6j*-type Cav2.1 channels often exhibited smaller peak currents than the wild-type channels, although no significant difference in the geometrical average peak current density at 0 mV was evident when the two channels were compared (Fig. 2A). The Ba^{2+} currents in the *6j*- and wild-type channels were similar in terms of their current–voltage relationships (Fig. 2B and C). Both channel currents were first detected at voltages near −30 mV and attained their maximal amplitudes at around 0 mV. Neither the activation nor inactivation curves differed significantly between the *6j*-type and wild-type channels (data not shown). A standard double-pulse protocol was applied, and data obtained during recovery from inactivation were fitted to a single exponential function (Fig. 2D and E). The *6j*-type channel currents recovered from inactivation more rapidly than did the wild-type currents. The

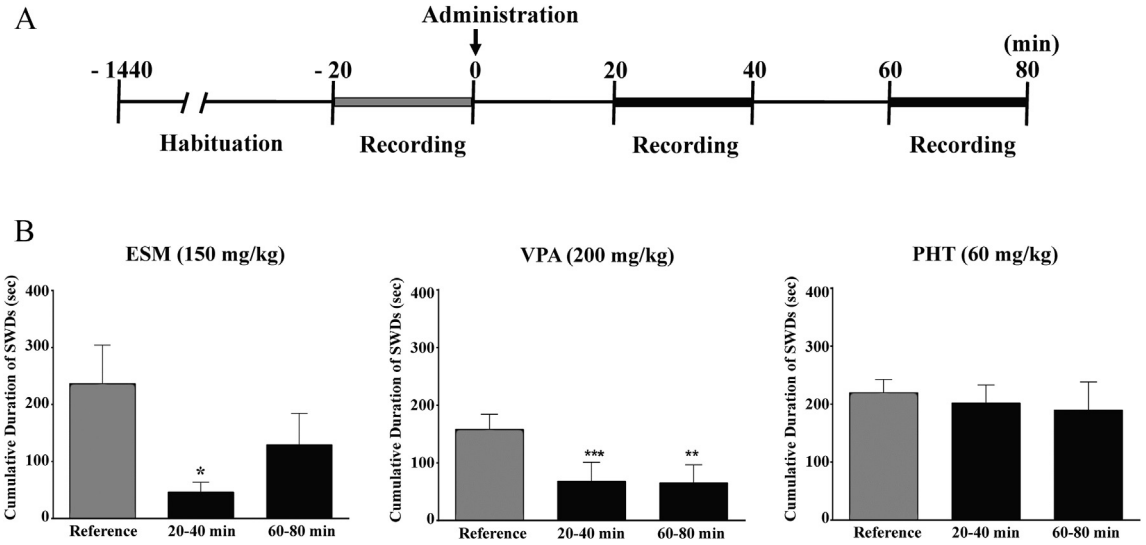

Fig. 4. Effects of antiepileptic drugs on *tottering-6j* mice. (A) The EEG recording schedule. Drugs were administered at 0 min in the experimental period (arrow). (B) Cumulative durations of SWDs in the 20-min intervals before and after drug administration. ESM: ethosuximide, VPA: valproic acid, PHT: phenytoin (all $n = 8$). $^{*}p < 0.05$, $^{**}p < 0.01$ and $^{***}p < 0.01$ compared with the reference animals (one-way repeated-measures ANOVA followed by Bonferroni's multiple comparison test).

recovery time constant ($\tau_{recovery}$) of the *6j*-type channel was significantly less than that of the wild-type channel.

3.3. Absence-like seizures of tottering-6j mice

To explore whether *tottering-6j* mice exhibited absence-like seizures, EEG and behavioral data were collected. *Tottering-6j* mice exhibited 5–8 Hz SWDs in the bilateral cortex, concomitant with sudden immobility and staring (Fig. 3A). Over 1-h observation periods of *tottering-6j* mice 35–39 weeks of age ($n = 5$), the mean number of SWDs was 206.80 ± 53.73. The mean duration of each SWD was 2.46 ± 0.13 s, and the cumulative duration of seizures in the 1 h was 550.33 ± 139.22 s. SWDs were also observed in the hippocampus, synchronous with those in the cortex (Fig. 3B).

3.4. Effects of antiepileptic drugs on absence-like seizures in tottering-6j mice

The effects of antiepileptic drugs on absence-like seizures in *tottering-6j* mice were examined using the protocol shown in Fig. 4. ESM significantly inhibited seizure development 20–40 min after administration and tended to inhibit SWD development 60–80 min after administration. VPA significantly inhibited SWD development at both 20–40 min and 60–80 min after administration. In contrast, PHT did not inhibit SWD development. Vehicle alone did not affect SWD occurrence in *tottering-6j* mice (data not shown).

4. Discussion

Knockout of *Cacna1a* in mice triggers absence-like seizures in addition to severe ataxia; such animals die 3–4 weeks after birth [7], suggesting that the Cav2.1 channel is indispensable. We first examined the expression pattern of mutant *Cacna1a* in the brain of *tottering-6j* mice. ISH did not reveal any difference in *Cacna1a* expression between the brains of wild-type and *tottering-6j* mice. We next examined mutant *Cacna1a* expression levels in the olfactory bulb, cerebral cortex, caudate putamen, hippocampus, and cerebellum of both strains and found no significant difference. Also, the gross cytoarchitecture of mutant brains appeared to be normal.

Several animals mutant in the *Cacna1a* gene have been reported, and comparison of allelic variants is helpful to clarify the relationships among various structural and physiological abnormalities, and observed behavioral deficits, and to allow us to understand how the channel functions. In the present study, EEG recordings and behavioral analyses revealed that *tottering-6j* mice exhibited SWD concomitant with sudden behavioral arrest, similar to the phenotypes of *Cacna1a* mutants, *rkr*, *tg*, and *tottering-4j* mice, and GRY rats [1,8]. None of *rol, wobby,* or *tottering-5* mice exhibits absence-like seizures [13–15]. The *rol, wobby,* and *tottering-5* mutations are located in the voltage sensor segment (S4) of domain III. The *rkr* and *tg* mutations are located close to the ion-selective pore-forming region of the extracellular segment lying between S5 and S6 of domains III and II, respectively [16,17]. The mutation in *tottering-4j* mice is located in the S5 region of domain II [13]. The *gry* mutation is a substitution of amino acid 215 in the extracellular segment lying between S5 and S6 of domain I [8]. The *tottering-6j* mutation lacks a part of the S4–S5 linker, S5, and part of the S5–S6 linker in domain I (amino acids 213–264) [9]. Such results indicate that the S5 and S5–S6 linker regions play critical roles in preventing absence-like seizures. Electrophysiological data from *tottering-6j*- and *gry*-type heterologous reconstitution expression systems yielded very similar results; recovery from inactivation was accelerated, but both the current density and the voltage dependence of activation and inactivation were unaffected. On the other hand, the SWD frequency (206.8 ± 53.73/h) in *tottering-6j* mice was higher that of GRY rats (28.8 ± 6.88/h). In terms of SWD duration, that of *tottering-6j* mice (2.46 ± 0.13 s) was shorter than that of GRY rats (9.58 ± 1.14 s). Data from heterologous recombinant expression systems cannot be simply generalized to native neurons because many other factors may affect the functions of mutant channels. Therefore, further work with native neurons is required to gain additional insights, and to allow us to understand the relationship between channel dysfunction and behavioral abnormality.

In humans, absence seizure is a nonconvulsive type of idiopathic generalized epilepsy, characterized by a brief loss of consciousness (the absence), and SWD evident on EEG during seizure activity [18]. Mutations in *CACNA1A* have been detected in humans experiencing absence seizures [19], suggesting that such mutations might be

involved in the generation of such seizures. The amino acid sequence including the S4–S5 linker, S5, and part of the S5–S6 linker is highly conserved among several vertebral species [13]. In humans, *CACNA1A* mutations are associated with three neurological disorders, FHM1, EA2, and SCA6. Interestingly, the missense mutations noted in FHM1 (amino acid 218) and EA2 (amino acids 248, 253, and 256) patients are located in the S4–S5 linker region and in the S5 and S5–S6 linker region of domain I, respectively [6]. Such results indicate that this region plays an important role in Cav2.1 functioning and that the *tottering-6j* mouse may be a useful model of hemiplegic migraine and episodic ataxia.

Animal models are essential not only to aid in the understanding of the pathogenesis of Cav2.1 channelopathies but also to evaluate antiepileptic drugs. The seizures were characterized by spontaneous and bilateral SWDs accompanied by immobility and staring. We found that the *tottering-6j* mouse exhibited absence-like seizures corresponding to those of humans. In humans, ESM effectively suppresses such seizures, and VPA effectively treats both absence seizures and tonic convulsions. On the other hand, PHT is effective against tonic convulsions but not against absence seizures. ESM and VPA are the first-line antiepileptic drugs recommended in the most commonly used guidelines [20]. In *tottering-6j* mice, ESM and VPA also inhibited both the development and duration of SWD, whereas PHT did not, suggesting that the pharmacological profile of the seizures of *tottering-6j* mice is very similar to that of absence seizures in humans. The presence of seizures in this mouse strain supports the association between *Cacna1a* mutation and absence seizures.

In conclusion, although further work is required to explain how the *tottering-6j* mutation alters the structure and function of the Cav2.1 channel in the neuronal network, eventually triggering seizures, we have shown in our present study that the *tottering-6j* mouse is a useful model of human absence epilepsy; the seizure ontogeny and the pharmacological properties are well defined. Also, the mouse may serve as a model for other *Cacna1a*-related diseases, including hemiplegic migraine and episodic ataxia.

Conflict of interest

None.

Acknowledgments

This work was supported by the National Basic Research Program of China (2011CB711003) to Weidong Li, and Grants-in-Aid for Scientific Research KAKENHI (22500396) to Eiki Takahashi.

Transparency document

Transparency document related to this article can be found online at http://dx.doi.org/10.1016/j.bbrc.2015.05.050.

References

[1] E. Takahashi, Cav2.1 channelopathy and mouse genetic approaches to investigate function and dysfunction of Cav2.1 channel, in: M. Yamaguchi (Ed.), Calcium Signaling, Nova Science Publishers, Inc., New York, 2012, pp. 149–158.
[2] A. Neely, P. Hidalgo, Structure-function of proteins interacting with the α1 pore-forming subunit of high-voltage-activated calcium channels, Front. Physiol. 5 (2014) 209.
[3] R.A. Ophoff, G.M. Terwindt, M.N. Vergouwe, R. van Eijk, P.J. Oefner, S.M. Hoffman, J.E. Lamerdin, H.W. Mohrenweiser, D.E. Bulman, M. Ferrari, J. Haan, D. Lindhout, G.J. van Ommen, M.H. Hofker, M.D. Ferrari, R.R. Frants, Familial hemiplegic migraine and episodic ataxia type-2 are caused by mutations in the Ca^{2+} channel gene CACNL1A4, Cell 87 (1994) 543–552.
[4] A.M. van den Maagdenberg, E.E. Kors, E.R. Brunt, W. van Paesschen, J. Pascual, D. Ravine, S. Keeling, K.R. Vanmolkot, F.L. Vermeulen, G.M. Terwindt, J. Haan, R.R. Frants, M.D. Ferrari, Episodic ataxia type 2. Three novel truncating mutations and one novel missense mutation in the CACNA1A gene, J. Neurol. 249 (2002) 1515–1519.
[5] O. Zhuchenko, J. Bailey, P. Bonnen, T. Ashizawa, D.W. Stockton, C. Amos, W.B. Dobyns, S.H. Subramony, H.Y. Zoghbi, C.C. Lee, Autosomal dominant cerebellar ataxia (SCA6) associated with small polyglutamine expansions in the alpha 1A-voltage-dependent calcium channel, Nat. Genet. 15 (1997) 62–69.
[6] D. Pietrobon, Cav2.1 channelopathies, Pflugers Arch. 460 (2010) 375–393.
[7] K. Jun, E.S. Piedras-Rentería, S.M. Smith, D.B. Wheeler, S.B. Lee, T.G. Lee, H. Chin, M.E. Adams, R.H. Scheller, R.W. Tsien, H.S. Shin, Ablation of P/Q-type Ca^{2+} channel currents, altered synaptic transmission, and progressive ataxia in mice lacking the alpha(1A)-subunit, Proc. Natl. Acad. Sci. U. S. A. 96 (1999) 15245–15250.
[8] S. Tokuda, T. Kuramoto, K. Tanaka, S. Kaneko, I.K. Takeuchi, M. Sasa, T. Serikawa, The ataxic groggy rat has a missense mutation in the P/Q-type voltage-gated Ca^{2+} channel alpha1A subunit gene and exhibits absence seizures, Brain Res. 1133 (2007) 168–177.
[9] W. Li, Y. Zhou, X. Tian, T.Y. Kim, N. Ito, K. Watanabe, A. Tsuji, K. Niimi, Y. Aoyama, T. Arai, E. Takahashi, New ataxic tottering-6j mouse allele containing a Cacna1a gene mutation, PLoS One 7 (2012) e44230.
[10] Y. Sakuraoka, T. Sawada, T. Shiraki, K. Park, Y. Sakurai, N. Tomosugi, K. Kubota, Analysis of hepcidin expression: in situ hybridization and quantitative polymerase chain reaction from paraffin sections, World J. Gastroenterol. 18 (2012) 3727–3731.
[11] E. Takahashi, K. Niimi, Spatial learning deficit bon aged heterozygous Cav2.1 channel mutant mice, *rolling* mouse Nagoya, Exp. Gerontol. 44 (2009) 274–279.
[12] A.H. Heller, M.A. Dichter, R.L. Sidman, Anticonvulsant sensitivity of absence seizures in the tottering mutant mouse, Epilepsia 24 (1983) 25–34.
[13] T. Miki, T.A. Zwingman, M. Wakamori, C.M. Lutz, S.A. Cook, D.A. Hosford, K. Herrup, C.F. Fletcher, Y. Mori, W.N. Frankel, V.A. Letts, Two novel alleles of tottering with distinct Cav2.1 calcium channel neuropathologies, Neuroscience 155 (2008) 31–44.
[14] Y. Mori, M. Wakamori, S. Oda, C.F. Fletcher, N. Sekiguchi, E. Mori, N.G. Copeland, N.A. Jenkins, K. Matsushita, Z. Matsuyama, K. Imoto, Reduced voltage sensitivity of activation of P/Q-type calcium channels is associated with the ataxic mouse mutation rolling Nagoya (tg(rol)), J. Neurosci. 20 (2000) 5654–5662.
[15] G. Xie, S.J. Clapcote, B.J. Nieman, T. Tallerico, Y. Huang, I. Vukobradovic, S.P. Cordes, L.R. Osborne, J. Rossant, J.G. Sled, J.T. Henderson, J.C. Roder, Forward genetic screen of mouse reveals dominant missense mutation in the P/Q-type voltage-dependent calcium channel, CACNA1A, Genes Brain Behav. 6 (2007) 717–727.
[16] C.F. Fletcher, C.M. Lutz, T.N. O'Sullivan Jr., J.D. Shaughnessy, R. Hawkes, W.N. Frankel, N.G. Copeland, N.A. Jenkins, Absence epilepsy in tottering mutant mice is associated with calcium channel defects, Cell 87 (1996) 607–617.
[17] T.A. Zwingman, P.E. Neumann, J.L. Noebels, K. Herrup, Rocker is a new variant of the voltage-dependent calcium channel gene Cacna1a, J. Neurosci. 21 (2001) 1169–1178.
[18] A. Lüttjohann, G. van Luijtelaar, Dynamics of networks during absence seizure's on- an2 offset in rodents and man, Front. Physiol. 6 (2015) 16.
[19] A. Gambardella, A. Labate, The role of calcium channel mutations in human epilepsy, Prog. Brain Res. 213 (2014) 87–96.
[20] V.D. Nunes, L. Sawyer, J. Neilson, G. Sarri, J.H. Cross, Diagnosis and management of the epilepsies in adults and children: summary of updated NICE guidance, BMJ 344 (2012) e281.